Simultaneous Intracranial EEG-fMRI Shows Inter-Modality Correlation in Time-Resolved Connectivity Within Normal Areas but Not Within Epileptic Regions

Ben Ridley, Jonathan Wirsich, Gaelle Bettus, Roman Rodionov, Teresa Murta, Umair Chaudhary, David Carmichael, Rachel Thornton, Serge Vulliemoz, Andrew Mcevoy, et al.

Full Title: *Simultaneous intracranial EEG-fMRI shows inter-modality correlation in time-resolved connectivity within normal areas but not within epileptic regions*

Authors: Ben Ridley[a,b], , Jonathan Wirsich[a,b,c], Gaelle Bettus[a,b,c], Roman Rodionov[d,e], Teresa Murta[d,f], Umair Chaudhary[d,e], David Carmichael[g], Rachel Thornton[d,e], Serge Vulliemoz[d,e,h], Andrew McEvoy[d,e,i], Fabrice Wendling[j,k], Fabrice Bartolomei[c,l], Jean-Philippe Ranjeva[a,b], Louis Lemieux[d,e], Maxime Guye[a,b]

Affiliations: [a] Aix-Marseille Univ, CNRS, CRMBM UMR 7339, Marseille, France [b] APHM, Hôpitaux de la Timone, CEMEREM, Marseille, France [c] Aix Marseille Univ, Inserm, INS, Institut de Neurosciences des Systèmes, Marseille, France [d]Institute of Neurology, University College London (UCL), London, UK, WC1N 3BG. [e]MRI Unit, Epilepsy Society, Buckinghamshire, UK, SL9 0RJ. [f]Institute for Systems and Robotics and Department of Bioengineering, Instituto Superior Técnico, Universidade de Lisboa, Lisboa, Portugal. [g]Institute of Child Health, UCL, London, UK, WC1E 6BT. [h]EEG and Epilepsy Unit, Neurology Clinic, University Hospitals and Faculty of Medicine of Geneva, Switzerland, CH-1211. [i]Department of Neurosurgery, National Hospital for Neurology and Neurosurgery, London, UK, WC1N 3BG. [j]INSERM, U1099, Rennes, F-35000, France. [k]Université de Rennes 1, LTSI, F-35000, France. [l]APHM, Hôpitaux de la Timone, Service de Neurophysiologie Clinique, Marseille, France

Author Email:ben.ridley@univ-amu.fr; jonathan.wirsich@univ-amu.fr; gaelle.bgimeno@gmail.com; r.rodionov@ucl.ac.uk; teresa.murta.11@ucl.ac.uk; umair.chaudhary@ucl.ac.uk; d.carmichael@ucl.ac.uk; Rachel.Thornton@gosh.nhs.uk; Serge.Vulliemoz@hcuge.ch; a.mcevoy@ucl.ac.uk; fabrice.wendling@univ-rennes1.fr; fabrice.bartolomei@ap-hm.fr; jean-phillipe.ranjeva@univ-amu.fr; louis.lemieux@ucl.ac.uk; maxime.guye@ap-hm.fr

Corresponding Author: Ben Ridley. **Address:** CEMEREM, 264 rue Saint-Pierre, Marseille, 13385, France. **Email:** ben.ridley@univ-amu.fr **Tel:** +33 (0) 4913388467 **Fax :** +33 (0) 491388461

Compliance with Ethical Standards: The authors declare no competing financial interests. The authors obtained written informed consent from all patients, in compliance with the ethical requirements of the Declaration of Helsinki and the Joint Research Ethics Committee of the NHNN (UCLH NHS Foundation Trust) and UCL Institute of Neurology.

Acknowledgements: Data for this was acquired at UCLH/UCL who received a proportion of funding from the Department of Health's NIHR Biomedical Research Centres funding scheme. Processing and analysis were undertaken at CRMBM/CEMEREM. This work was also supported with funds from the Swiss National Science Foundation (141165 and 140332, SPUM Epilepsy).

Abstract

For the first time in research in humans, we used simultaneous icEEG-fMRI to examine the link between connectivity in haemodynamic signals during the resting-state (rs) and connectivity derived from electrophysiological activity in terms of the inter-modal connectivity correlation (IMCC). We quantified IMCC in 9 patients with drug-resistant epilepsy i) within brain networks in 'healthy' non-involved cortical zones (NIZ) and ii) within brain networks involved in generating seizures and interictal spikes (IZ1) or solely spikes (IZ2). Functional connectivity (h^2) estimates for 10 minutes of resting-state data were obtained between each pair of electrodes within each clinical zone for both icEEG and fMRI. A sliding window approach allowed us to quantify the variability over time of h^2 (vh^2) as an indicator of connectivity dynamics. We observe significant positive IMCC for h^2 and vh^2, for multiple bands in the NIZ only, with the strongest effect in the lower icEEG frequencies. Similarly, intra-modal h^2 and vh^2 were found to be differently modified as a function of different epileptic processes: compared to NIZ, h^2_{BOLD} was higher in IZ1, but lower in IZ2, while h^2_{icEEG} showed the inverse pattern. This corroborates previous observations of inter-modal connectivity discrepancies in pathological cortices, while providing the first direct invasive and simultaneous comparison in humans. We also studied time-resolved FC variability multimodally for the first time, finding that IZ1 shows both elevated internal h^2_{BOLD} and less rich dynamical variability, suggesting that its chronic role in epileptogenesis may be linked to greater homogeneity in self-sustaining pathological oscillatory states.

Keywords: connectivity; multimodal imaging; resting-state; focal epilepsy; dynamic connectivity

Abbreviations:

ECoG – Electrocorticography
FC – Functional Connectivity
FLE – Frontal Lobe Epilepsy
IED – Interictal Epileptic Discharges
icEEG – Intracranial Electroencephalography
ICN – Intrinsic Connectivity Network
IZ – Irritative Zone
NIZ – Non-involved Zone
TLE – Temporal Lobe Epilepsy
SEEG – stereo-electroencephalography

1. INTRODUCTION

The advent of multimodal approaches for investigating brain activity, and the range of methods for quantifying oscillatory phenomena in the resting-state, provide both the potential for novel insight and novel challenges. Interpretation of scalp EEG-fMRI data is complicated by the fact that scalp EEG is affected by conductively inhomogeneous head tissue, and is limited in relation to buried structures (Carmichael, Vulliemoz et al. 2012). Pre-surgical evaluation in drug-resistant epilepsies commonly involves implantation of electrodes (Rosenow and Luders 2001). Thus, this population proffers a unique opportunity to investigate the relationship between haemodynamic and electrophysiological phenomena in both 'healthy' regions not involved in epileptic activity and regions subject to paroxysmal pathology, via an invasive method not normally permissible in human samples.

Intracranial EEG (icEEG) is the gold standard for categorising cortices in terms of epileptogenicity and involves the implantation of electrodes in the form of subdural grids or strips for electrocorticography (ECoG) and/or stereo-electroencephalography (SEEG) via depth electrodes (Rosenow and Lüders 2001). For example, icEEG can be used to define and categorise the set of brain regions involved in the generation of paroxysmal interictal epileptiform discharges (IEDs), called the Irritative Zone (IZ) (Chauvel 2001; Palmini 2006; Bartolomei et al. 2016). The IZ can be further sub-divided into the IZ1, involved in generating seizure (ictal) activity as well as IEDs, and the IZ2, exclusively involved in the generation of IEDs.

In recent years, conventional functional brain-mapping has been complemented by resting-state functional connectivity (rsFC) – the analysis of statistical interdependencies in the spontaneous time courses of activity between remote regions – as a means of understanding the role of networks in distributed function in normal and pathological brains (Guye et al. 2008; Sporns 2014; Raichle 2015). Functional connectivity analyses in controls have revealed macro-scale intrinsic connectivity networks (ICNs) (Smith et al. 2009). In epilepsy, rsFC analyses have been applied to both such anatomically-defined ICNs, in addition to clinically-determined networks that vary anatomically from patient to patient but are unified in terms of the disease processes they manifest, such as IZ1 and IZ2 (Guye et al. 2010; Laufs 2012; Centeno and Carmichael 2014). The hope is that FC analyses in the interictal resting-state, with their limited demands on patients and without the need to wait for unpredictable ictal and inter-ictal activity, can facilitate the understanding of epilepsy in the both the lab and clinic. While substantial study has been made of changes to ICNs, less has been done to understand clinically-defined epileptic networks via the rsFC paradigm. Often taking advantage of the spatial resolution and whole brain coverage of fMRI, such studies have indicated distributed changes including both augmented and impaired connectivity with links to pathological and potentially compensatory processes in epilepsy (Bettus et al. 2009; Bettus et al. 2010; Zhang et al. 2010; Centeno

and Carmichael 2014; Holmes et al. 2014; Ridley et al. 2015). While region of interest (ROI) selection in such studies may be motivated by an understanding of the likely candidates for involvement in epileptogenesis [cf. Bettus et al., 2009], they may still fail to account for individual variation in the actual location and extent of pathological activity. A small number of studies have taken advantage of the greater specificity of icEEG relative to *a priori* regions of interest when parcellating cortices into irritative and physiological/non-involved zones (NIZ) to explore functional connectivity specifically as a function of involvement in different epileptic processes in the interictal resting-state (Bartolomei et al., 2013; Bartolomei et al., 2013; Bettus et al., 2008; Schevon et al., 2007; Warren et al., 2010). Such studies indicate increased functional connectivity as measured by icEEG (icEEG-FC) in regions involved in interictal epileptiform activity in comparison to spared cortices.

To our knowledge, Bettus et al. (2011) is the only study to have used the specificity of the icEEG gold standard in parallel with BOLD-derived FC estimates from the same location, within the same individuals. These authors showed an apparent inter-modality discrepancy: higher FC as revealed by icEEG and lower FC as measured by BOLD in electrophysiologically abnormal regions. However, since both modalities were not acquired simultaneously, confounding inter-session effects cannot be ruled out as an explanation. For example, impacts arising from the time of day of acquisition, emotional/mental state (including sleep) and consumption of pharmacological agents such as caffeine or nicotine have been shown to effect connectivity (Duncan and Northoff 2013). Furthermore, variation in connectivity over time has recently become a target of interest as possibly physiological signal reflecting the dynamic formation and integration of functional and dysfunctional assemblies (Tagliazucchi and Laufs 2015). Epilepsy is recognized as involving modifications on multiple time scales, not only chronic modifications to structural and functional networks (Spencer 2002; Laufs 2012; Bartolomei et al. 2013b). Like seizures, IEDs may impact connectivity intermittently and on timescales smaller than the several minutes generally averaged over in 'static' functional connectivity estimates (Centeno and Carmichael 2014; Lopes et al. 2014). While the biophysical underpinnings remain unclear, variance in resting BOLD signal oscillations is spatially organized (Kaneoke et al. 2012), and the modulation of its standard deviation between cognitive states is modulated by age and processing speed (Garrett et al. 2013), suggesting that it is a biologically informative feature and more than mere noise (Garrett et al. 2010) . Similarly, the variation of FC induced by non-stationarities during the resting-state/interictal period is starting to be investigated via sliding window analyses in the context of epilepsy (Laufs et al. 2014; Douw et al. 2015; Nedic et al. 2015). These indicate a modification in the variability of FC in regions with plausible *a priori* relationships to seizure generation and semiology. The advent of simultaneous icEEG-fMRI (Carmichael et al. 2010; Vulliemoz et al. 2011; Carmichael et al. 2012) offers the possibility of

verifying this 1) within invasively *confirmed* epileptic regions and 2) ensuring the equal incidence of non-stationarities via the only means possible: simultaneous acquisition.

Here we take advantage of simultaneously acquired icEEG-fMRI data to study functional connectivity with the benefit of both greater specificity of separation of cortices in terms of disease process involvement and the exclusion of inter-session effects and differences in non-stationarities. Greater multimodal agreement in the current work would suggest previously observed multimodal discrepancies are due to intersession effects, while the contrary case would implicate 'genuine' differences in the signals being measured and/or their relationships. Extending this to time-resolved variability in FC, allows us to characterise the range of variability in normal regions, and whether the repertoire of functions states is impacted differentially by chronic exposure to different kinds of epileptic activity. Leveraging simultaneous icEEG-fMRI for the first time in the interictal resting state, we aimed to explore the strength and the multimodal relationships of FC and its variance, both in physiological regions not involved in epileptic processes (NIZ) as well as in diseased regions (IZ).

2. MATERIALS AND METHODS

2.1. Subjects

Nine (three female, mean age 30.4rs±4.5yrs, range 24-38yrs) subjects with drug-resistant epilepsy undergoing presurgical evaluation for resective surgery gave their informed consent to take part in this study, which was approved by the Joint Research Ethics Committee of the National Hospital for Neurology and Neurosurgery (NHNN, UCLH NHS Foundation Trust) and UCL Institute of Neurology, London, UK. See **Table 1** for full demographic information. All patients were recruited, monitored long-term and received simultaneous icEEG-fMRI at the NHNN, Queen Square, London, UK

2.2. Intracranial electrode implantation and categorization

Intracranial electrodes were implanted under general anaesthesia to test clinical hypotheses about the localization of epileptogenic regions. Following implantation, the patients underwent a CT scan to permit precise localisation of icEEG electrodes. Patients were then monitored in-clinic for an extended period to gather information regarding ictal and interictal pathological activity using icEEG. This information was used to characterize each electrode as belonging to a zone involved by different epileptic processes.

The epileptogenic/primary irritative zone (IZ1), the secondary irritative zone (IZ2), and the non-involved zone (NIZ) were determined for each patient, following Bettus et al (2011). IZ1 was defined as the subset of brain regions involved in the generation of seizures which may also exhibited interictal epileptic discharges (IEDs). IZ2 was defined as those regions only secondarily involved in seizures and which produce interictal spikes. Finally, NIZ were defined as structures without epileptiform discharges during clinical monitoring. After this monitoring period, the simultaneous icEEG-fMRI acquisitions analysed below were obtained within the 24 hours prior to electrode removal.

Grids or strips of electrodes were placed on the cortical surface, or penetrated the brain via multi-contact depth electrode leads. Grids were 4mm diameter disks with 2.3 mm diameter exposures, made of 90% platinum, 10% iridium. Depth electrodes were made of platinum and were either 0.9 or 1.1mm in diameter, and 2.3 or 2.4 mm in length. Within a given array, electrodes were spaced at intervals of 10mm for ECoG/grids/strips and 5mm or 10mm for depth. In situ, and across all arrays and individual implantation schemes, the mean inter-electrode Euclidean distance was 44±24mm. **Figure 1** depicts the position of electrodes and their labelling for each participant. For a detailed account of the clinical implantation targets and implanted electrodes see **Supporting Information S1**.

2.3. Resting-state simultaneous icEEG-fMRI acquisition and pre-processing

During 10 minutes of simultaneous icEEG-fMRI acquisition, patients were requested to lie at rest with their eyes open. MRI data were acquired using a 1.5 T Siemens Avanto scanner (Siemens, Erlangen, Germany) running software version VB15, with a quadrature head transmit–receive RF coil using low specific absorption rate (SAR) sequences (≤0.1 W/kg head average). The following scans were performed: 1) localiser, 2) FLASH T1-volume (TR:3s/TE: 40 ms/flip angle: 90°), 3) a GE-EPI fMRI resting-state scan (TR: 3s/TE: 78 ms/38 slices/200 volumes, 3×3×3 mm voxels). BOLD-FC data were pre-processed using SPM8 software (UCL Wellcome Trust Centre, London, UK). After slice-timing correction, images were realigned before spatial normalization (16 non-linear registration 7x6x7 basis functions) and smoothing (8 mm). Detrending and filtering (0.01-0.08 Hz) were applied using the REST SPM8 toolbox. Sources of spurious or regionally non-specific variance related to physiological artefacts were removed via regression of signals from manually defined ROIs in the lateral ventricles and deep cerebral white matter using SPM's 'Marsbar' toolbox. Maximum framewise displacement (mm) in 3 translational and rotational planes (degrees of arc converted to millimetres of displacement as per Power et al (2012)) did not exceed 1mm in any patient (average maximum displacement (mm) across patients: x: 0.09, y: 0.13 , z: 0.28, pitch: 0.17, roll: 0.12, yaw: 0.13).

Following co-registration of the post-operative CT scan and T2* images with the T1 (normalized mutual information, SPM8) a 5mm radius spherical ROI was defined for each electrode contact. Given the cortical surface placement of grid contacts, and the wish to ensure only neural signals were captured by ROIs, grid-derived spherical ROIs were placed normal to and entirely submerged under the cortical surface immediately adjacent to the corresponding electrode contact. A ROI fMRI signal time course was extracted by averaging the pre-processed fMRI over the ROI's voxels from T2* images.

icEEG signals from subsets of the implanted electrodes (henceforth called *recording electrodes*) were recorded using an MR-compatible amplifier system (Brain Products, Munich, Germany) and dedicated recording software (*Brain Vision Recorder*) as described in Vulliemoz et al. (2011) and Carmichael et al. (2012) during the fMRI scans. Recording electrodes were selected based on the interpretation of the clinical recordings in order to focus on the channels of greatest scientific interest given the work involved in connecting the electrodes to the MRI-compatible system and, in some patients, due to the smaller number of channels available in the MRI-compatible amplifier compared to the number of implanted electrodes. The EEG recording system (0.5 μV amplitude resolution) - sampling at 5 kHz - was synchronised to the scanner's 20 kHz gradient clock, with subsequent filtering and down-sampling to 250 Hz. Scanning-related artifacts were removed using standard implementation of template subtraction and filtering (Allen et al. 2000) in the *Brain Vision*

Analyzer software (V1.3). Data was analysed after subtracting the common average reference (minimum number of electrodes included: 30, P01), and filtered according to several frequency ranges of interest: broadband (0.5-100Hz), Delta (0.5-3.4 Hz); Theta (3.4-7.4 Hz); Alpha (7.4-12.4 Hz); Beta (12.4-24 Hz); and Gamma (24-100 Hz).

While every recording electrode was used to define an ROI, the icEEG and fMRI data were subject to visual inspection by experts [GB and FB] and overly noisy and likely artifactual timeseries of either modality were excluded from all analyses. Using this approach, 13 leads/ROIs were rejected (6 grid electrodes from P03 and one depth from P06 due to icEEG data, and 6 grid electrodes from P06 due to BOLD data) and 570 were retained. **Table 2** provides a breakdown of the number of ROIs provided for the final analysis by each patient.

2.4 Functional connectivity analysis

A nonlinear measure of covariance, h^2, was used to estimate functional connectivity between every pair of electrodes. See Wendling et al. (2010) for an in depth account of this metric. Briefly, dependency between two signals *X* and *Y* derived from the same modality was quantified using:

$$h^2(\tau) = 1 - \frac{VAR[\frac{Y(t+\tau)}{X(t)}]}{VAR[Y(t+\tau)]}$$

With

$$VAR\left[\frac{Y(t+\tau)}{X(t)}\right] \triangleq \arg\min_{h}\left(E\left[Y(t+\tau) - h\big(X(t)\big)\right]^2\right)$$

where *h* is a nonlinear fitting curve which approximates the relationship between *X* and *Y* and *t* is the time shift that maximizes the value of the h^2 coefficient.

Conceptually, h^2 is a normalized non-linear correlation coefficient which quantifies the reduction of variance in *Y* when *X* is used to predict *Y* samples. When $h^2_{XY}=1$, *Y* is fully determined by *X*, and $h^2_{XY}=0$ when no relationship exists between the two signals. While it is known that non-linearities can occur in EEG signals especially in epilepsy (Casdagli et al. 1997; van Diessen et al. 2015), the relative importance of being able to detect linear and non-linear components of relationships between signals is a subject of ongoing discussion (Netoff et al. 2004; Wendling et al. 2010). Note that h^2 is a measure of amplitude/power covariance and indicates the presence and strength of relationships (and does not, *per se*, differentiate between 'correlations' and 'anticorrelations'), with the advantage of not making any assumptions regarding their nature - linear or otherwise (Wendling et al. 2010). Additionally, the use of h^2 allows comparison with our previous findings in non-simultaneous recordings (Bettus et al. 2011).

h^2 values between pairs of electrodes or ROIs were computed over sliding window analyses, separately for each modality. When computing h^2_{icEEG} between electrodes a 5s window moving with 0.5s increments was used, while for computing h^2_{BOLD} between ROIs a 90s window moving with 2s increments was used. Window size was motivated by the need to be large enough to include uncorrelated (in time) *X*-*Y* values in order to compute a meaningful correlation, and on the assumption that 50 uncorrelated couples of *X*-*Y* values are needed for reliably computing the h^2 coefficient. Taking the auto-correlation function for EEG to be 100ms (Wendling et al. 2001), 50 samples provides a 5 second window size. 1.8 seconds was taken to be sufficient to include minimal autocorrelation given evidence that the autocorrelation coefficient of resting-state BOLD oscillations (TR=3s) in healthy controls drops of sharply after one second and reaches zero on the order of two seconds, and 50 samples yields a 90 second window (Kaneoke et al. 2012).

The h^2 values were averaged across windows over the entire scanning period time in order to get a single estimate of static functional connectivity (h^2). Additionally, the variation of h^2 over time (vh^2) was computed as the standard deviation of the h^2 estimates for each window across the entire run. An estimate of h^2 and vh^2 was obtained for BOLD, and for broadband and five sub-bands for icEEG signals. A thresholding procedure outlined in **Supporting Information 2** was used to verify that all pairwise relationships constituted evidence for the existence of a correlation between variables of interest at the 99% level of confidence.

In order to take advantage of a pre-existing module of the AMADEUS software (Wendling et al. 2010; Wendling 2015) - designed to compute large sets of pairwise h^2 - for our BOLD data and to ensure equivalency of processing it was necessary to resample BOLD data at 250 Hz using a 1-dimensional 1st order linear interpolation routine available in Matlab (interp1). This is identical to the procedure employed by Bettus et al. (2011), who also demonstrated the comparability of h^2 estimates on highly sampled and normal data.

2.5 Other metrics: IED count and inter-electrode distance

IEDs counts were calculated automatically with AMADEUS following Bourien et al (2005). The approach involves detecting abrupt increases (high amplitude, short duration spikes) in the mean value of the squared modulus of the signal when passed through a wavelet filter bank, enhancing the fast sharp component of the IED relative to the surrounding background EEG. A single IED count was associated with each pairwise interaction between electrodes by taking the average of the individual electrode spike counts. It should be noted that this automated procedure does not differentiate between paroxysmal activity of different types, and these automatic estimates of IEDs are distinct from those obtained manually during extended clinical monitoring and used to define clinical zones.

Euclidean distances (mm) were calculated between the centres of each ROI as a proxy for inter-electrode distances *in situ*.

2.6 Statistical comparisons

The following statistical analyses were performed using JMP version 9 (SAS Institute Inc., Cary, NC) on pairwise interactions between electrode/ROIs within the same clinical zone (IZ1, IZ2, NIZ). Relationships between pairs in different zones were not considered. **Table 2** provides information regarding the number of pairwise interactions provided within each zone, yielding an overall sample of n=11543.

We were also interested in the extent to which connectivity estimates derived from within each modality are associated between modalities. We assessed the inter-modal connectivity correlation (IMCC) via Pearson's r between the sample of pairwise connectivity estimates obtained from BOLD ROIs (h^2_{BOLD}) on the one hand, and the sample of pairwise connectivity estimates derived from icEEG electrodes (h^2_{icEEG}; broadband plus five sub-bands) on the other. The same procedure was applied between vh^2_{BOLD} and vh^2_{icEEG}. Correlation of h^2_{BOLD} and vh^2_{BOLD} in relation to IEDs was also considered. Thus IMCC was investigated for each of the three clinically-defined zones, and considered significant at a Bonferroni-corrected level of $0.05/((6+1)*3)=p<0.002$.

Differential impacts of clinically-defined zones on mean h^2 and vh^2 was modelled (ANOVA) using 'zone' as regressor of interest (3 levels) while controlling for several sources of 'spurious' variation. Two categorical covariates were included: 'Patient' (9 levels) and 'Electrode Type' (2 levels), the latter reflecting a departure with Bettus et al. (2008; 2011) in which patients were implanted solely with depth electrodes as in P01, P04 and P09 here, but unlike P06 implanted solely with grids and all other patients who had a mixture of depth and grid electrodes. Two continuous covariates, 'IEDs' and 'Euclidean distance' were also included, to account for other possible sources of variability inherent in the spatial sampling and incidence of paroxysmal activity in epileptic networks. Tests were compared to two thresholds for significance: an exploratory level of $p<0.05$, and on the assumption of multimodal associations a Bonferroni correction of the number of modalities (BOLD plus six icEEG bands) threshold of $0.05/7=p<0.007$.

3. RESULTS

3.1 Inter-modal connectivity correlations for h^2 and vh^2

Table 3 lists the observed correlation coefficients and associated p-values**.** In non-involved (NIZ) cortices, h^2_{BOLD} was significantly positively associated with both h^2 and vh^2 of all frequency bands measured by our icEEG data. IMCC was strongest in the slower icEEG bands, and weakest at the highest frequencies studied here. h^2_{BOLD} was negatively correlated with vh^2_{BOLD}. A negative association was also exhibited between vh^2_{BOLD} and vh^2_{icEEG} in the alpha, beta and gamma bands.

IMCC as observed in the non-involved region was not found in pathological cortices: no significant relationships were observed between h^2_{BOLD} and h^2_{icEEG} outside of the NIZ with the exception of the delta band in IZ1. Similarly, the only relationship between vh^2_{icEEG} and vh^2_{BOLD} in epileptic cortices was a positive correlation observed in the alpha band in IZ2. Finally, while negative correlations between h^2_{BOLD} and vh^2_{BOLD} were found in all zones, this negative relationship was stronger in pathological regions, substantially so for IZ1.

Pathological regions also demonstrated relationships not found in unaffected regions. In particular, significant aberrant negative correlations were found between h^2_{icEEG} and vh^2_{BOLD} in all icEEG bands, with the effects being strongest at the highest frequencies.

Finally, IEDs were found to be positively correlated with vh^2_{BOLD} in IZ2, while correlating with h^2_{BOLD} in IZ1.

3.2 Impact of zone on unimodal h^2 and vh^2

While accounting for confounding covariates, significant main effects (Bonferroni-corrected) of zone were observed on both h^2 and vh^2 for BOLD and across all sub-bands for icEEG-FC (**Table 4**). Post-hoc t-tests indicated a differential impact of epileptic processes on FC as well as disjunction in this impact depending on modality (**Tables 5-6, Figure 2, top**). In particular, IZ1 demonstrated higher h^2_{BOLD}, and IZ2 lower h^2_{BOLD} compared to NIZ, while for h^2_{icEEG} the inverse pattern was found across most bands. Across modalities, regions responsible for generating seizures (IZ1) exhibited the most variance in terms of their respective level of augmentation or disruption relative to the other zones (**Figure 3, left & right**) and IZ2 exhibited a more consistent relationship with the other zones (**Figure 3, middle**) of elevated h^2_{icEEG} and reduced h^2_{BOLD}. This discrepancy between modalities was also reflected in their variability over the sliding window time series (**Figure 2, bottom**), with pathological regions exhibiting elevated vh^2_{icEEG}, and lower vh^2_{BOLD}.

4. DISCUSSION

The current work confirms a previously observed discrepancy between icEEG- and BOLD-derived FC findings (h^2) (Bettus et al. 2008; Bettus et al. 2011) and extends it to FC variability over time (vh^2); in addition, we shed new light on the differential impact of different epileptic processes. We demonstrate for the first time using simultaneously acquired icEEG-fMRI that epileptic cortices are distinguished by their internal multimodal resting-state FC as a function of their involvement in different, clinically-relevant epileptic processes. Furthermore, we provide the first evidence that the inter-modal connectivity correlation that exists in unaffected regions may be modified in cortices affected by epileptic pathology, when estimating h^2 and vh^2 in unaffected regions and using invasive and simultaneous electrophysiological and haemodynamic signals.

4.1 Inter-modal connectivity correlation in physiological and pathological cortices

The non-invasive BOLD signal is an indirect measure of neurological activity, motivating interest in better understanding its electrophysiological correlates, including in terms of icEEG-derived connectivity and its relationship to both spontaneous BOLD activity and resting-state functional connectivity. Correlates from electrophysiological activity (as opposed to connectivity) at multiple spatial and temporal scales have been proposed (Keilholz 2014; Tagliazucchi and Laufs 2015), with both high-frequency local field potentials (Shmuel and Leopold 2008; Nir et al. 2008; Schölvinck et al. 2010), and lower frequencies (Lu et al. 2007; He et al. 2008; Pan et al. 2013; Lu et al. 2016) being advanced as electrophysiological correlates of spontaneous rsfMRI fluctuations. Others have examined the extent to which connectivity estimates derived from EEG and BOLD are associated with one another, in terms of the intermodal correlation of the connectivity estimates derived from each modality. Invasive electrophysiological recordings in rats indicate relationships between BOLD correlations and EEG band power correlations that are strongest in lower frequency bands, especially delta, but extending to gamma (Lu et al. 2007; Pan et al. 2011). Modulation by exogenous stimulation of rsfMRI functional connectivity in rat whisker barrel cortex has been found to be reflected in the delta range, but not at higher frequencies (Lu et al. 2016). In humans, it has been shown that BOLD covariance (functional connectivity) matrices can be well explained based on EEG covariance matrices - similarly so across bands - while the reverse is only true in the lower frequency bands (Deligianni et al. 2014). Here, in the first study to combine invasive electrophysiological recording and simultaneous fMRI acquisition, we observe correlations between FC estimated on haemodynamic and electrophysiological signals across frequency bands in non-involved, 'healthy' cortex (**Table 3**). We find the strongest relationships at lower frequencies, possibly reflecting a bias toward lower bands in maintaining relationships over distant regions due to the relationship between distance and signal delay (Schölvinck et al. 2013).

In contrast, we find almost no evidence of the inter-modality correlation observed in NIZ for h^2 and vh^2 estimates in IZ1 and IZ2. One possibility is that each modality captures a different aspect of the functional reorganization of networks in the context of epilepsy (Bettus et al. 2010; Bettus et al. 2011; Duncan et al. 2013; Bartolomei et al. 2013b). In this scheme, slow (<0.1Hz) BOLD signal fluctuations may reflect perturbance of the functional integrity of macro-level intrinsic networks, and the faster and broader frequency range of EEG to abnormal organisation of epileptic networks poised to evolve into hypersynchrony at the onset of seizures (Bartolomei et al. 2013a; Bartolomei et al. 2013b) or interictal activity (Centeno and Carmichael 2014). Modification of FC within regions characterised by involvement in specifically epileptic processes is supported by icEEG (Schevon et al. 2007; Bettus et al. 2008; Bartolomei et al. 2013a; Bartolomei et al. 2013b) and fMRI (Bettus et al. 2011). Additionally, networks thought to reflect intrinsic pattern of connectivity (ICNs), are also subject to a variety of modifications in epilepsy (Centeno and Carmichael 2014). An apparent dissociation between interictal electrophysiological and haemodynamic metrics of connectivity in focal epileptic regions was indicated by Bettus and colleagues (2011) when analysing non-simultaneous data acquired from the same individuals. They found evidence for a diminution of functional connectivity within the IZ2 as measured by BOLD, and an augmentation in h^2_{icEEG} within IZ1 and IZ2 which was significant in the beta band. Here, using simultaneously-acquired icEEG-fMRI, we confirm this inter-modality discrepancy in connectivity estimates (**Figure 2, top**), as well as extending it to the dynamic variability of FC estimates over time (**Figure 2, bottom**). In fMRI studies investigating connectivity in epilepsy, where 'involved' regions are selected on the *a priori* basis of being likely candidates for involvement in epileptogenesis, a common finding is a reduction in BOLD-FC (Centeno and Carmichael 2014) . To our knowledge, Bettus et al. (2011) is the only study to have used the specificity of the icEEG gold standard in parallel with BOLD-derived FC estimates from the same location within the same individuals, and observe a trend to BOLD-FC reduction in the IZ1 versus NIZ, though it is non-significant. Interestingly, while an inter-modality discrepancy is also observed in the current results for IZ1, it points in an opposite direction than these limited antecedents might lead one to expect: an augmentation of BOLD-FC and reduction in icEEG-FC (**Figure2, top**). While studies that examine BOLD-FC between ICN nodes typically report decreases in patients, modifications within nodes tell a more complicated story. Not only decreases but increases in connectivity are evident in the frontal and temporal nodes of multiple ICNs, both for TLE (He et al. 2008; Liao et al. 2010) and FLE (Braakman et al. 2013; Widjaja et al. 2013). Though increases have been interpreted as potentially compensatory (Bettus et al. 2009; Bettus et al. 2010; Ridley et al. 2015), FC increases have also been associated with worse neuropsychological outcomes (Holmes et al. 2014). In epileptic networks, increases have been seen in the regional homogeneity of resting BOLD oscillations (Mankinen et al. 2011), and indeed there appears to be a pattern of

connectivity increases reported when it is specifically the vicinity of individually localized epileptogenic regions under consideration. Stufflebeam et al. (2011) found BOLD-FC increases in local (<5mm) connectivity in proximity to grid electrodes classified as belonging to the seizure onset zone in 5 of 6 patients with focal epilepsy. Similarly, Luo et al. (2014) reported an enhancement of FC in FLE patients in the immediate neighbourhood of cortical epileptogenic zones defined by EEG-fMRI data fusion.

We note that the variability in findings observed across the literature in 'epileptogenic' regions is reflected in the inter-individual variability of FC estimates (**Figure 3, left**) and differences between IZ1 and non-involved zones in our sample (**Figure 3, right**). Insofar as modifications to connectivity in epileptic networks which are salient to different modalities might reflect different disease process, as suggested above, the extent to which these might interact with different aetiologies is unknown, and is an area that should receive further attention. Indeed, a recent analysis of magnetoencephalography data in both mesial TLE and focal neocortical patients indicates a mixture of focal increases and decreases in pre-surgery FC in epileptogenic regions that would later undergo resection (putative IZ1) versus non-involved homologous regions in the contralateral hemisphere (Englot et al. 2015). In contrast, the IZ2 may represent a more similar situation across individuals than IZ1 (**Figure 3**, IZ2-NIZ contrast), as relatively 'healthy' cortex extending beyond focal lesions that is not so degenerate as to self-generate seizures, and where IEDs are the main form of pathological activity impinging on brain networks. For example, while metabolic abnormalities suggestive of defective neurovascular coupling are observed in IZ2 (Guye et al. 2002; Guye et al. 2005), they are reversible as seen in post-operative patients who have become seizure free after successful resection surgery (Serles et al. 2001). This difference in the relationship to ongoing disease processes may be reflected in the fact that IEDs appear to be disruptive to h^2_{BOLD} connectivity leading to its reduction in IZ2 (**Figure 2, top**) and greater variability as measured by vh^2_{icEEG} (**Figure 2, bottom** and **Table 2**), versus the positive correlation observed between IEDs and vh^2_{BOLD} and the anti-correlation of vh^2_{BOLD} and h^2_{icEEG} (**Table 3**).

4.2 Altered neurovascular coupling in pathological cortices

Altered neurovascular coupling has been proposed as an explanation of apparent discrepancies between icEEG- and BOLD-derived indices of FC (Bettus et al. 2011), and might also play a role in the absence of correlation seen here. Metabolic anomalies in electrophysiologically abnormal regions have been demonstrated in both TLE (Guye et al. 2002) and FLE (Guye et al. 2005), with the addition of both vascularisation defects (Duncan 2010) and blood-brain barrier dysfunctions in TLE (Oby and Janigro 2006). Furthermore, evidence from rat models suggests that neurovascular coupling is comparable between evoked and spontaneous BOLD oscillations (Bruyns-

Haylett et al. 2013), but that evoked neurovascular coupling is modified during ictal epileptic activity (Harris et al. 2013). This is suggestive of a broad comparability between spontaneous and evoked neurovascular coupling which may be subject to modification in the context of epilepsy.

Our results suggest that multimodal differences persist despite an equivalent *incidence* of inter-modal between-session factors (as ensured by simultaneous acquisition), though this in itself does not exclude a difference in *impact* between modalities. Modelling may be one means of understanding how such differences contribute to the discrepancies seen here, but it should be noted that the choice of parameters derived from one signal for the understating of another is highly non-trivial. For example, an argument for a disruptive effect of interictal epileptic transients such as IEDs on connectivity has a *prima facie* plausibility. However, empirical results have been more equivocal with negative (Nissen et al. 2016), positive (Bartolomei et al. 2013a) and null (Bettus et al. 2008) associations of IEDs with FC in epileptics networks observed in scalp and invasive electrophysiology, but also overall limited-to-no-effect of removing IED-containing epochs by censoring data (Bettus et al. 2008; Warren et al. 2010b; Bartolomei et al. 2013a). On the other hand, general linear modelling of IEDs and other epileptic transient provided some of the earliest evidence of an interaction of epilepsy with resting-state phenomena in the form of IED- and seizure-associated BOLD changes in regions associated with intrinsic connectivity networks, most especially the default mode network (Gotman and Pittau 2011; van Graan et al. 2015). Interictal phenomena may be associated with increases, decreases or unchanged BOLD signal (Bénar et al., 2006; Salek-Haddadi et al., 2006; Stefan and Lopes da Silva, 2013; Thornton et al., 2011), and BOLD changes may be found in regions with no apparent involvement on EEG (Kobayashi et al. 2006). Interpreting the variability of these results is further complicated by recent evidence that coupling is state- and time-dependant in addition to being spatially organized in the resting-state (Feige et al. 2016). While suggestive of a framework for understanding the differential impact between modalities, how altered coupling might pertain to the findings in the current study - the focus of which is FC in epileptic networks rather than resting activity in ICNs per se - is unclear. Indeed, there is evidence of dissociation between different means of characterizing resting state activity in epilepsy, with discordant finding in terms of the amplitude and connectivity of resting state activity in the same patients (Zhang et al. 2015). As noted above, multiple processes that contribute to neurovascular coupling and hence the BOLD-signal generation cascade are effected in epilepsy, and as such represent sources of unmodeled noise standing between underlying processes and the signals as estimated via such metrics as (de-)activation or connectivity. The separate contributions of perfusion deficits (Duncan 2009) and altered metabolic demands in the chronic epileptic state and under the specific influence of epileptic transients will likely need to be characterized. Multimodal exploration as traditionally performed and in new combinations is one tool

to mutually constrain different sources of non-neuronal noise and mutually support conclusions by filling in missing information (Uludağ and Roebroeck 2014).

4.3 Multimodal relationships of time varying FC

In addition to establishing a relationship between indices of connectivity in simultaneous icEEG and fMRI data, sliding window analyses allowed us to resolve the variability of connectivity over time. Comparable analyses have been applied previously to fMRI data in temporal lobe epilepsy patients, showing modifications in time-resolved connectivity associated with disease burden of memory scores (Douw et al. 2015), and both increases (Laufs et al. 2014) and decreases (Nedic et al. 2015) in the variability of FC in regions that might plausibly be considered part of epileptic networks on an *a priori* basis. Current results, in regions assigned to IZ1 and IZ2 by the electrophysiological gold standard, tend to agree with the latter: vh^2_{BOLD} is significantly reduced in IZ1 (**Figure 2**). Furthermore, we provide the first simultaneous icEEG-fMRI evidence in humans of an inter-modality discrepancy in the variability of FC over time in epileptic regions: in opposition to BOLD, vh^2 estimates derived from icEEG indicate an augmentation across bands in irritative regions, and specifically in IZ1 in alpha, beta and gamma bands.

Our findings indicate that in healthy cortex BOLD h^2 is related to vh^2_{icEEG} across sub-bands, but that BOLD vh^2 shows a relationship to icEEG vh^2 only in alpha, beta and gamma bands (**Table 3**). Both findings may reflect the imbalance when trying to predict FC in one modality from the other (Deligianni et al. 2014), with variability in all icEEG bands imparting information about BOLD connectivity oscillations, but the inverse not being the case. This is in good agreement with previous work indicating covariation in correlation between modalities in comparable bands in rat and macaque studies (Magri et al. 2012; Thompson et al. 2013), and possibly reflects the widely hypothesized role of alpha and gamma bands in particular in communication between neural assemblies at distal and local scales, respectively (Keilholz 2014). As with multimodal relationships between estimates of connectivity, multimodal relationships in the variability in FC across sliding window timeseries appear to be disrupted in pathological cortices in epilepsy.

Whole brain computational simulation approaches comparing empirical data to simulated functional data derived from structural models suggest that the agreement between simulated and empirical data are best when both a low energy spontaneous state and several states of localized high activity are stable states of the system (Cabral et al. 2014). In this context, slow resting-state oscillations represent the dynamic exploration of the different states of the brain's intrinsic functional repertoire instigated by underlying anatomic connectivity and intrinsic noise (Deco and Jirsa 2012). This could maintain the brain in a state of heightened competition ready to evolve momentarily into a specific state under the influence of internal or external sensory modulation (Deco and Corbetta

2011). Our results show that IZ1 is associated with both an augmentation of h^2_{BOLD} and a reduction in vh^2_{BOLD}. This could reflect a dynamic repertoire that is reduced in diseased cortices under the influence of both epileptogenic processes and paroxysmal interictal activity, with a propensity toward seizures being one of the states that such influences promote. If a reduced repertoire reflects homogeneity in self-sustaining pathological oscillatory states, this could be reflected in both abnormally high FC and less rich dynamics, consistent with the negative relationship between h^2 and vh^2 of BOLD which we find to be augmented in irritative cortices and at its highest in IZ1. In contrast, IZ2 may represent cortex that is less degenerate in this sense – showing no reduction in vh^2_{BOLD} compared to NIZ – but is chronically subject to disruption by interictal transients which could be reflected in the correlation of IEDs and vh^2_{BOLD} (**Table 3**).

4.4. Limitations and Future Directions

The implantation, placement and coverage of intracranial electrodes are motivated first and foremost by clinical necessity, leading to a degree of heterogeneity in our sample. We have attempted to identify and account for several forms of heterogeneity via quantitative proxies including Euclidean distance and automatically-generated IED counts. For example, since the automatic extraction of IEDs is based on locating abrupt and transient signal modulations there is a possibility of misidentifying non-pathological transients as IEDs, as is also the case for manually defined IEDs (Noachtar and Rémi 2009). **Supplementary Figure 1** shows the number of 'IEDs' identified by zone at group and individual levels, and though the relative amounts of 'IEDs' detected by the algorithm meet clinical expectations (Bartolomei et al. 2016), a small amount were located in regions classified as NIZ based on experienced clinical analysis. It is likely that these proxies account for only some of the variance involved in estimating connectivity in epilepsy, and more exact measures of propagation distance and a more discerning treatment of different types of interictal electrophysiological phenomena may provide further insights. Additionally, a development of the current work could involve the normalization of BOLD-FC against estimates derived from controls using the ROIs extracted from the electrodes in each patient, to allow the demarcation of differences deriving from spatial sampling and pathology. Other potential influences on FC could be considered as well, including anti-epileptic medications as patients were continued on their normal regimen and were not reduced at the time of scan

While simultaneously acquired icEEG-fMRI has the benefit of avoiding the confound of separate acquisitions, it is not without its own technical challenges (Carmichael et al. 2010; Carmichael et al. 2012). In particular, reduction in BOLD signal can occur around electrodes due to the difference in magnetic susceptibility between electrode and tissue in the presence of the scanner's strong magnetic field. A validation study by Carmichael and colleagues (Carmichael et al. 2012)

found that signal reduction was similar for depth and grid electrodes, and was on average less than 50% at 5mm from the electrode, the radius of the ROIs used here. Similarly, data from simultaneous EEG-fMRI studies suggests minimal disturbances of temporal signal to noise ratios, with comparable detectability of activation fMRI time-courses in the presence and absence of EEG recording acquisition during fMRI (Luo and Glover 2012). Given the points of consistency our BOLD results share with previous non-simultaneous icEEG-fMRI and unimodal fMRI data (Bettus et al. 2009; Bettus et al. 2011; Mankinen et al. 2011; Stufflebeam et al. 2011; Luo et al. 2014), signal drop-out due to electrodes seems unlikely to be a crucial factor in this work. Our results tend to suggest that despite the loss of MRI signal in the immediate vicinity of the electrodes, the observed effects extend to a large enough brain area beyond the region of drop out around each electrode.

Finally, while we have examined the variability of FC over time for a sliding window analysis, it should be acknowledged that establishing true dynamics requires a demonstration of a distinction with random fluctuations, and that this is particularly controversial in the context of fluctuations in BOLD-derived FC (Keilholz 2014). That said, we demonstrate relationships between haemodynamic and electrophysiological indices of variation and connectivity suggesting that at least some part of the fluctuation in BOLD connectivity reflects a neural origin.

5. Conclusion

We provide the first evidence derived from intracranial EEG and simultaneous BOLD signals of inter-modality correlation in healthy human cortex in terms of both static functional connectivity and its time-resolved variability. Furthermore, while ruling out differences in the intra-individual incidence of non-stationarities, we observe a lack of inter-modality connectivity correlation in regions subject to epileptic processes, with a confirmation of inter-modality discrepancies in functional connectivity associated with epileptic cortices while establishing for the first time that this discrepancy extends to the dynamical variability of connectivity over time.

References

Allen PJ, Josephs O, Turner R (2000) A method for removing imaging artifact from continuous EEG recorded during functional MRI. NeuroImage 12:230–239. doi: 10.1006/nimg.2000.0599

Bartolomei F, Bettus G, Stam CJ, Guye M (2013a) Interictal network properties in mesial temporal lobe epilepsy: A graph theoretical study from intracerebral recordings. Clin Neurophysiol Off J Int Fed Clin Neurophysiol. doi: 10.1016/j.clinph.2013.06.003

Bartolomei F, Guye M, Wendling F (2013b) Abnormal binding and disruption in large scale networks involved in human partial seizures. EPJ Nonlinear Biomed Phys 1:1–16. doi: 10.1140/epjnbp11

Bartolomei F, Trébuchon A, Bonini F, et al (2016) What is the concordance between the seizure onset zone and the irritative zone? A SEEG quantified study. Clin Neurophysiol Off J Int Fed Clin Neurophysiol 127:1157–1162. doi: 10.1016/j.clinph.2015.10.029

Bettus G, Bartolomei F, Confort-Gouny S, et al (2010) Role of resting state functional connectivity MRI in presurgical investigation of mesial temporal lobe epilepsy. J Neurol Neurosurg Psychiatry 81:1147–1154. doi: 10.1136/jnnp.2009.191460

Bettus G, Guedj E, Joyeux F, et al (2009) Decreased basal fMRI functional connectivity in epileptogenic networks and contralateral compensatory mechanisms. Hum Brain Mapp 30:1580–1591. doi: 10.1002/hbm.20625

Bettus G, Ranjeva J-P, Wendling F, et al (2011) Interictal functional connectivity of human epileptic networks assessed by intracerebral EEG and BOLD signal fluctuations. PloS One 6:e20071. doi: 10.1371/journal.pone.0020071

Bettus G, Wendling F, Guye M, et al (2008) Enhanced EEG functional connectivity in mesial temporal lobe epilepsy. Epilepsy Res 81:58–68. doi: 10.1016/j.eplepsyres.2008.04.020

Bourien J, Bartolomei F, Bellanger JJ, et al (2005) A method to identify reproducible subsets of co-activated structures during interictal spikes. Application to intracerebral EEG in temporal lobe epilepsy. Clin Neurophysiol Off J Int Fed Clin Neurophysiol 116:443–455. doi: 10.1016/j.clinph.2004.08.010

Braakman HMH, Vaessen MJ, Jansen JFA, et al (2013) Frontal lobe connectivity and cognitive impairment in pediatric frontal lobe epilepsy. Epilepsia 54:446–454. doi: 10.1111/epi.12044

Bruyns-Haylett M, Harris S, Boorman L, et al (2013) The resting-state neurovascular coupling relationship: rapid changes in spontaneous neural activity in the somatosensory cortex are associated with haemodynamic fluctuations that resemble stimulus-evoked haemodynamics. Eur J Neurosci 38:2902–2916. doi: 10.1111/ejn.12295

Cabral J, Kringelbach ML, Deco G (2014) Exploring the network dynamics underlying brain activity during rest. Prog Neurobiol 114:102–131. doi: 10.1016/j.pneurobio.2013.12.005

Carmichael DW, Thornton JS, Rodionov R, et al (2010) Feasibility of simultaneous intracranial EEG-fMRI in humans: a safety study. NeuroImage 49:379–390. doi: 10.1016/j.neuroimage.2009.07.062

Carmichael DW, Vulliemoz S, Rodionov R, et al (2012) Simultaneous intracranial EEG-fMRI in humans: protocol considerations and data quality. NeuroImage 63:301–309. doi: 10.1016/j.neuroimage.2012.05.056

Casdagli MC, Iasemidis LD, Savit RS, et al (1997) Non-linearity in invasive EEG recordings from patients with temporal lobe epilepsy. Electroencephalogr Clin Neurophysiol 102:98–105.

Centeno M, Carmichael DW (2014) Network connectivity in epilepsy: resting state fMRI and EEG–fMRI contributions. Epilepsy 5:93. doi: 10.3389/fneur.2014.00093

Chauvel P (2001) Contributions of Jean Talairach and Jean Bancaud to epilepsy surgery. In: Luders H, Comair YG (eds) Epilepsy Surgery. Lippincott Williams & Wilkins, Philadelphia, pp 35–41

Deco G, Corbetta M (2011) The dynamical balance of the brain at rest. Neurosci Rev J Bringing Neurobiol Neurol Psychiatry 17:107–123. doi: 10.1177/1073858409354384

Deco G, Jirsa VK (2012) Ongoing cortical activity at rest: criticality, multistability, and ghost attractors. J Neurosci Off J Soc Neurosci 32:3366–3375. doi: 10.1523/JNEUROSCI.2523-11.2012

Deligianni F, Centeno M, Carmichael DW, Clayden JD (2014) Relating resting-state fMRI and EEG whole-brain connectomes across frequency bands. Front Neurosci 8:258. doi: 10.3389/fnins.2014.00258

Douw L, Leveroni CL, Tanaka N, et al (2015) Loss of resting-state posterior cingulate flexibility is associated with memory disturbance in left temporal lobe epilepsy. PloS One 10:e0131209. doi: 10.1371/journal.pone.0131209

Duncan D, Duckrow RB, Pincus SM, et al (2013) Intracranial EEG evaluation of relationship within a resting state network. Clin Neurophysiol Off J Int Fed Clin Neurophysiol 124:1943–1951. doi: 10.1016/j.clinph.2013.03.028

Duncan J (2009) The current status of neuroimaging for epilepsy. Curr Opin Neurol 22:179–184. doi: 10.1097/WCO.0b013e328328f260

Duncan JS (2010) Imaging in the surgical treatment of epilepsy. Nat Rev Neurol 6:537–550. doi: 10.1038/nrneurol.2010.131

Duncan NW, Northoff G (2013) Overview of potential procedural and participant-related confounds for neuroimaging of the resting state. J Psychiatry Neurosci JPN 38:84–96. doi: 10.1503/jpn.120059

Englot DJ, Hinkley LB, Kort NS, et al (2015) Global and regional functional connectivity maps of neural oscillations in focal epilepsy. Brain J Neurol 138:2249–2262. doi: 10.1093/brain/awv130

Feige B, Spiegelhalder K, Kiemen A, et al (2016) Distinctive time-lagged resting-state networks revealed by simultaneous EEG-fMRI. NeuroImage. doi: 10.1016/j.neuroimage.2016.09.027

Garrett DD, Kovacevic N, McIntosh AR, Grady CL (2013) The modulation of BOLD variability between cognitive states varies by age and processing speed. Cereb Cortex N Y N 1991 23:684–693. doi: 10.1093/cercor/bhs055

Garrett DD, Kovacevic N, McIntosh AR, Grady CL (2010) Blood oxygen level-dependent signal variability is more than just noise. J Neurosci Off J Soc Neurosci 30:4914–4921. doi: 10.1523/JNEUROSCI.5166-09.2010

Gotman J, Pittau F (2011) Combining EEG and fMRI in the study of epileptic discharges. Epilepsia 52 Suppl 4:38–42. doi: 10.1111/j.1528-1167.2011.03151.x

Guye M, Bartolomei F, Ranjeva J-P (2008) Imaging structural and functional connectivity: towards a unified definition of human brain organization? Curr Opin Neurol 21:393–403. doi: 10.1097/WCO.0b013e3283065cfb

Guye M, Bettus G, Bartolomei F, Cozzone PJ (2010) Graph theoretical analysis of structural and functional connectivity MRI in normal and pathological brain networks. Magma N Y N 23:409–421. doi: 10.1007/s10334-010-0205-z

Guye M, Le Fur Y, Confort-Gouny S, et al (2002) Metabolic and electrophysiological alterations in subtypes of temporal lobe epilepsy: a combined proton magnetic resonance spectroscopic imaging and depth electrodes study. Epilepsia 43:1197–1209.

Guye M, Ranjeva JP, Le Fur Y, et al (2005) 1H-MRS imaging in intractable frontal lobe epilepsies characterized by depth electrode recording. NeuroImage 26:1174–1183. doi: 10.1016/j.neuroimage.2005.03.023

Harris S, Bruyns-Haylett M, Kennerley A, et al (2013) The effects of focal epileptic activity on regional sensory-evoked neurovascular coupling and postictal modulation of bilateral sensory processing. J Cereb Blood Flow Metab Off J Int Soc Cereb Blood Flow Metab 33:1595–1604. doi: 10.1038/jcbfm.2013.115

He BJ, Snyder AZ, Zempel JM, et al (2008) Electrophysiological correlates of the brain's intrinsic large-scale functional architecture. Proc Natl Acad Sci U S A 105:16039–16044. doi: 10.1073/pnas.0807010105

Holmes M, Folley BS, Sonmezturk HH, et al (2014) Resting state functional connectivity of the hippocampus associated with neurocognitive function in left temporal lobe epilepsy. Hum Brain Mapp 35:735–744. doi: 10.1002/hbm.22210

Kaneoke Y, Donishi T, Iwatani J, et al (2012) Variance and autocorrelation of the spontaneous slow brain activity. PloS One 7:e38131. doi: 10.1371/journal.pone.0038131

Keilholz SD (2014) The neural basis of time-varying resting-state functional connectivity. Brain Connect 4:769–779. doi: 10.1089/brain.2014.0250

Kobayashi E, Bagshaw AP, Grova C, et al (2006) Negative BOLD responses to epileptic spikes. Hum Brain Mapp 27:488–497. doi: 10.1002/hbm.20193

Laufs H (2012) Functional imaging of seizures and epilepsy: evolution from zones to networks. Curr Opin Neurol 25:194–200. doi: 10.1097/WCO.0b013e3283515db9

Laufs H, Rodionov R, Thornton R, et al (2014) Altered FMRI connectivity dynamics in temporal lobe epilepsy might explain seizure semiology. Front Neurol 5:175. doi: 10.3389/fneur.2014.00175

Liao W, Zhang Z, Pan Z, et al (2010) Altered functional connectivity and small-world in mesial temporal lobe epilepsy. PloS One 5:e8525. doi: 10.1371/journal.pone.0008525

Lopes R, Moeller F, Besson P, et al (2014) Study on the Relationships between Intrinsic Functional Connectivity of the Default Mode Network and Transient Epileptic Activity. Front Neurol 5:201. doi: 10.3389/fneur.2014.00201

Lu H, Wang L, Rea WW, et al (2016) Low- but Not High-Frequency LFP Correlates with Spontaneous BOLD Fluctuations in Rat Whisker Barrel Cortex. Cereb Cortex N Y N 1991 26:683–694. doi: 10.1093/cercor/bhu248

Lu H, Zuo Y, Gu H, et al (2007) Synchronized delta oscillations correlate with the resting-state functional MRI signal. Proc Natl Acad Sci U S A 104:18265–18269. doi: 10.1073/pnas.0705791104

Luo C, An D, Yao D, Gotman J (2014) Patient-specific connectivity pattern of epileptic network in frontal lobe epilepsy. NeuroImage Clin 4:668–675. doi: 10.1016/j.nicl.2014.04.006

Luo Q, Glover GH (2012) Influence of dense-array EEG cap on fMRI signal. Magn Reson Med 68:807–815. doi: 10.1002/mrm.23299

Magri C, Schridde U, Murayama Y, et al (2012) The amplitude and timing of the BOLD signal reflects the relationship between local field potential power at different frequencies. J Neurosci Off J Soc Neurosci 32:1395–1407. doi: 10.1523/JNEUROSCI.3985-11.2012

Mankinen K, Long X-Y, Paakki J-J, et al (2011) Alterations in regional homogeneity of baseline brain activity in pediatric temporal lobe epilepsy. Brain Res 1373:221–229. doi: 10.1016/j.brainres.2010.12.004

Nedic S, Stufflebeam SM, Rondinoni C, et al (2015) Using network dynamic fMRI for detection of epileptogenic foci. BMC Neurol 15:262. doi: 10.1186/s12883-015-0514-y

Netoff TI, Pecora LM, Schiff SJ (2004) Analytical coupling detection in the presence of noise and nonlinearity. Phys Rev E Stat Nonlin Soft Matter Phys 69:017201. doi: 10.1103/PhysRevE.69.017201

Nir Y, Mukamel R, Dinstein I, et al (2008) Interhemispheric correlations of slow spontaneous neuronal fluctuations revealed in human sensory cortex. Nat Neurosci 11:1100–1108.

Nissen IA, van Klink NEC, Zijlmans M, et al (2016) Brain areas with epileptic high frequency oscillations are functionally isolated in MEG virtual electrode networks. Clin Neurophysiol Off J Int Fed Clin Neurophysiol 127:2581–2591. doi: 10.1016/j.clinph.2016.04.013

Noachtar S, Rémi J (2009) The role of EEG in epilepsy: a critical review. Epilepsy Behav EB 15:22–33. doi: 10.1016/j.yebeh.2009.02.035

Oby E, Janigro D (2006) The blood-brain barrier and epilepsy. Epilepsia 47:1761–1774. doi: 10.1111/j.1528-1167.2006.00817.x

Palmini A (2006) The concept of the epileptogenic zone: a modern look at Penfield and Jasper's views on the role of interictal spikes. Epileptic Disord Int Epilepsy J Videotape 8 Suppl 2:S10-15.

Pan W-J, Thompson G, Magnuson M, et al (2011) Broadband local field potentials correlate with spontaneous fluctuations in functional magnetic resonance imaging signals in the rat somatosensory cortex under isoflurane anesthesia. Brain Connect 1:119–131. doi: 10.1089/brain.2011.0014

Pan W-J, Thompson GJ, Magnuson ME, et al (2013) Infraslow LFP correlates to resting-state fMRI BOLD signals. NeuroImage 74:288–297. doi: 10.1016/j.neuroimage.2013.02.035

Power JD, Barnes KA, Snyder AZ, et al (2012) Spurious but systematic correlations in functional connectivity MRI networks arise from subject motion. NeuroImage 59:2142–2154. doi: 10.1016/j.neuroimage.2011.10.018

Raichle ME (2015) The restless brain: how intrinsic activity organizes brain function. Philos Trans R Soc Lond B Biol Sci. doi: 10.1098/rstb.2014.0172

Ridley BGY, Rousseau C, Wirsich J, et al (2015) Nodal approach reveals differential impact of lateralized focal epilepsies on hub reorganization. NeuroImage 118:39–48. doi: 10.1016/j.neuroimage.2015.05.096

Rosenow F, Lüders H (2001) Presurgical evaluation of epilepsy. Brain J Neurol 124:1683–1700.

Schevon CA, Cappell J, Emerson R, et al (2007) Cortical abnormalities in epilepsy revealed by local EEG synchrony. NeuroImage 35:140–148. doi: 10.1016/j.neuroimage.2006.11.009

Schölvinck ML, Leopold DA, Brookes MJ, Khader PH (2013) The contribution of electrophysiology to functional connectivity mapping. NeuroImage 80:297–306. doi: 10.1016/j.neuroimage.2013.04.010

Schölvinck ML, Maier A, Ye FQ, et al (2010) Neural basis of global resting-state fMRI activity. Proc Natl Acad Sci U S A 107:10238–10243. doi: 10.1073/pnas.0913110107

Serles W, Li LM, Antel SB, et al (2001) Time course of postoperative recovery of N-acetyl-aspartate in temporal lobe epilepsy. Epilepsia 42:190–197.

Shmuel A, Leopold DA (2008) Neuronal correlates of spontaneous fluctuations in fMRI signals in monkey visual cortex: Implications for functional connectivity at rest. Hum Brain Mapp 29:751–761. doi: 10.1002/hbm.20580

Smith SM, Fox PT, Miller KL, et al (2009) Correspondence of the brain's functional architecture during activation and rest. Proc Natl Acad Sci U S A 106:13040–13045. doi: 10.1073/pnas.0905267106

Spencer SS (2002) Neural networks in human epilepsy: evidence of and implications for treatment. Epilepsia 43:219–227.

Sporns O (2014) Contributions and challenges for network models in cognitive neuroscience. Nat Neurosci 17:652–660. doi: 10.1038/nn.3690

Stufflebeam SM, Liu H, Sepulcre J, et al (2011) Localization of focal epileptic discharges using functional connectivity magnetic resonance imaging. J Neurosurg 114:1693–1697. doi: 10.3171/2011.1.JNS10482

Tagliazucchi E, Laufs H (2015) Multimodal imaging of dynamic functional connectivity. Front Neurol 6:10. doi: 10.3389/fneur.2015.00010

Thompson GJ, Merritt MD, Pan W-J, et al (2013) Neural correlates of time-varying functional connectivity in the rat. NeuroImage 83:826–836. doi: 10.1016/j.neuroimage.2013.07.036

Uludağ K, Roebroeck A (2014) General overview on the merits of multimodal neuroimaging data fusion. NeuroImage 102 Pt 1:3–10. doi: 10.1016/j.neuroimage.2014.05.018

van Diessen E, Numan T, van Dellen E, et al (2015) Opportunities and methodological challenges in EEG and MEG resting state functional brain network research. Clin Neurophysiol Off J Int Fed Clin Neurophysiol 126:1468–1481. doi: 10.1016/j.clinph.2014.11.018

van Graan LA, Lemieux L, Chaudhary UJ (2015) Methods and utility of EEG-fMRI in epilepsy. Quant Imaging Med Surg 5:300–312. doi: 10.3978/j.issn.2223-4292.2015.02.04

Vulliemoz S, Carmichael DW, Rosenkranz K, et al (2011) Simultaneous intracranial EEG and fMRI of interictal epileptic discharges in humans. NeuroImage 54:182–190. doi: 10.1016/j.neuroimage.2010.08.004

Warren CP, Hu S, Stead M, et al (2010a) Synchrony in normal and focal epileptic brain: the seizure onset zone is functionally disconnected. J Neurophysiol 104:3530–3539. doi: 10.1152/jn.00368.2010

Warren CP, Hu S, Stead M, et al (2010b) Synchrony in normal and focal epileptic brain: the seizure onset zone is functionally disconnected. J Neurophysiol 104:3530–3539. doi: 10.1152/jn.00368.2010

Wendling F (2015) Software Amadeus-Visualisation. Inserm-Université de Rennes 1. FR.001.420017.000.S.P.2015.000.31230

Wendling F, Bartolomei F, Bellanger JJ, Chauvel P (2001) [Identification of epileptogenic networks from modeling and nonlinear analysis of SEEG signals]. Neurophysiol Clin Clin Neurophysiol 31:139–151.

Wendling F, Chauvel P, Biraben A, Bartolomei F (2010) From intracerebral EEG signals to brain connectivity: identification of epileptogenic networks in partial epilepsy. Front Syst Neurosci 4:154. doi: 10.3389/fnsys.2010.00154

Widjaja E, Zamyadi M, Raybaud C, et al (2013) Abnormal functional network connectivity among resting-state networks in children with frontal lobe epilepsy. AJNR Am J Neuroradiol 34:2386–2392. doi: 10.3174/ajnr.A3608

Xia M, Wang J, He Y (2013) BrainNet Viewer: A Network Visualization Tool for Human Brain Connectomics. PLoS ONE. doi: 10.1371/journal.pone.0068910

Zhang Z, Lu G, Zhong Y, et al (2010) fMRI study of mesial temporal lobe epilepsy using amplitude of low-frequency fluctuation analysis. Hum Brain Mapp 31:1851–1861. doi: 10.1002/hbm.20982

Zhang Z, Xu Q, Liao W, et al (2015) Pathological uncoupling between amplitude and connectivity of brain fluctuations in epilepsy. Hum Brain Mapp 36:2756–2766. doi: 10.1002/hbm.22805

Figure Legends

Fig.1 Regions of interest (ROIs) Schematic representation of individual implantation schemes projected onto templates in MNI space. Red spheres: ROIs in the primary irritative zone (IZ1); yellow spheres: ROIs in secondary irritative zone (IZ2); black spheres: ROIs in non-involved zone (NIZ). Created using BrainNet Viewer (Xia et al. 2013)

Fig.2 Post-hoc t-contrasts between zones in terms of functional connectivity (top) and variability (bottom) Values correspond to adjusted means accounting for covariates other than zone. Error bars correspond to standard error of the mean. Bb, Broadband. Dark grey indicates a test significant at $p<0.05$, solid black indicates significance at a Bonferroni-corrected level of $p<0.007$.

Fig.3 Inter-individual variability in connectivity metrics and inter-zone contrasts

Boxplots of inter-individual variability in h^2 (top) and vh2 (bottom). Inter-individual estimates in mean (Left) estimates, and contrasts between zones (right). Note the distribution of data for the contrast IZ1-NIZ around zero for Δh^2 across modalities.

Figure

Click here to download Figure Fig1.tif

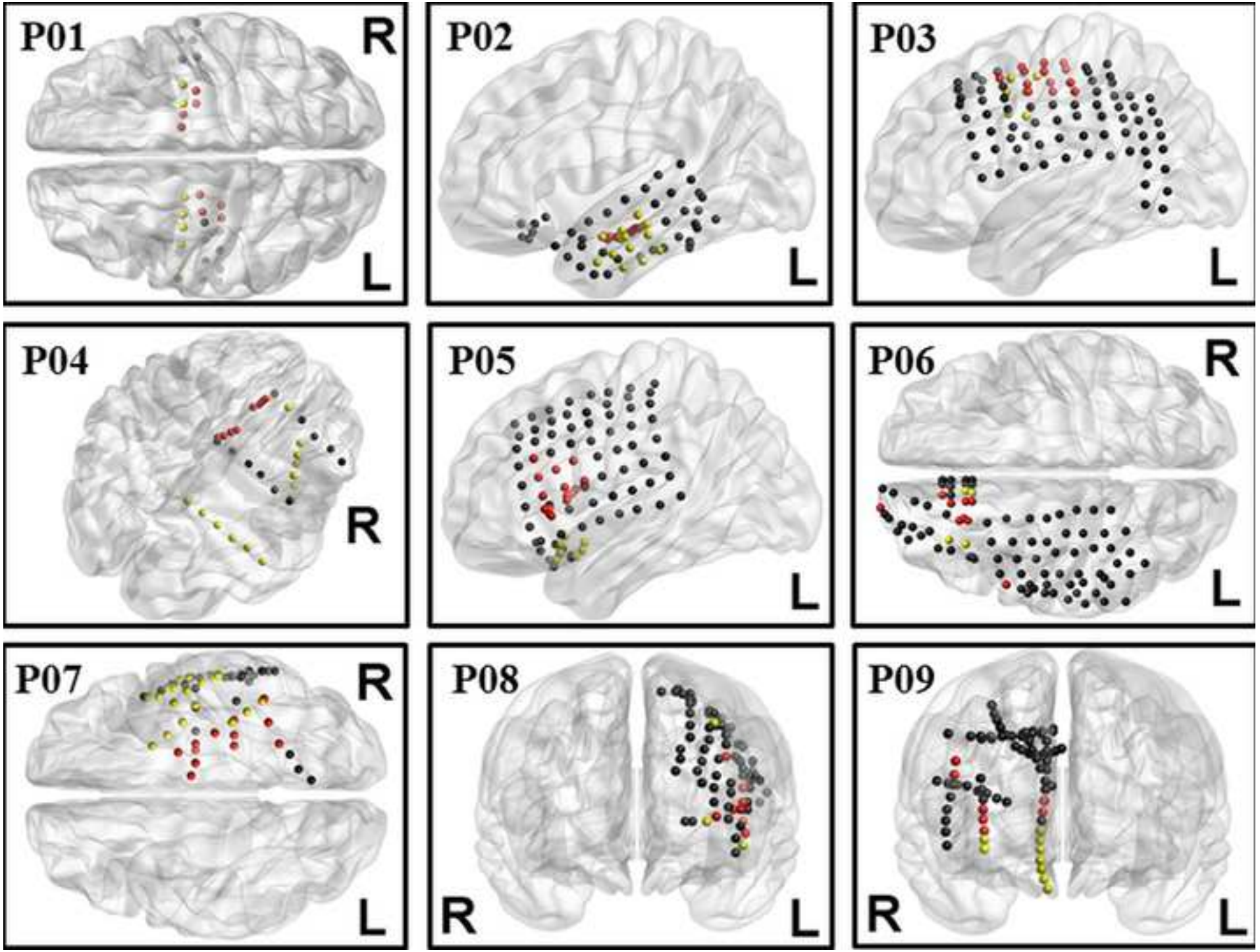

Figure

Click here to download Figure Fig2.tif

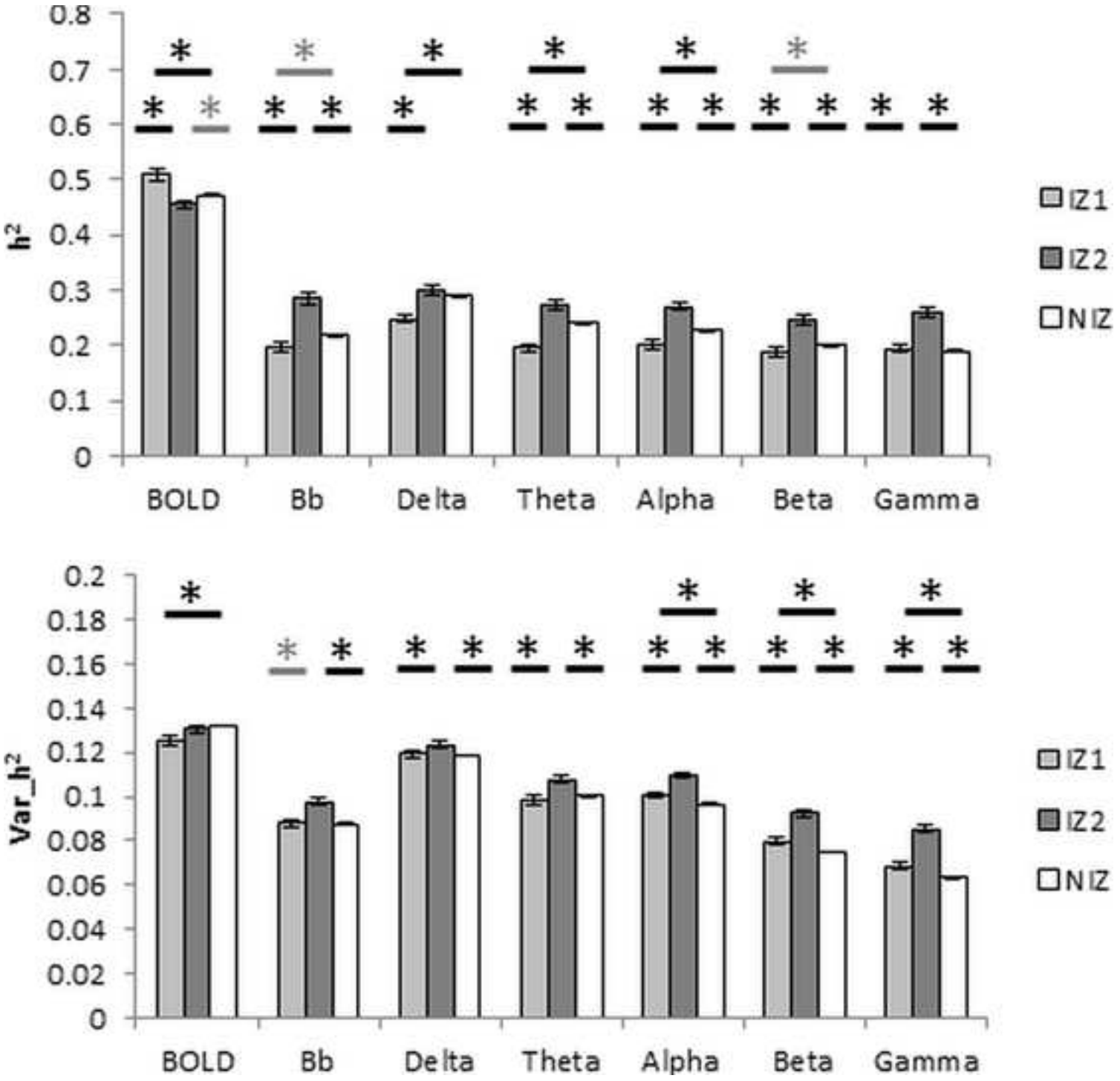

Figure

Click here to download Figure Fig3.tif

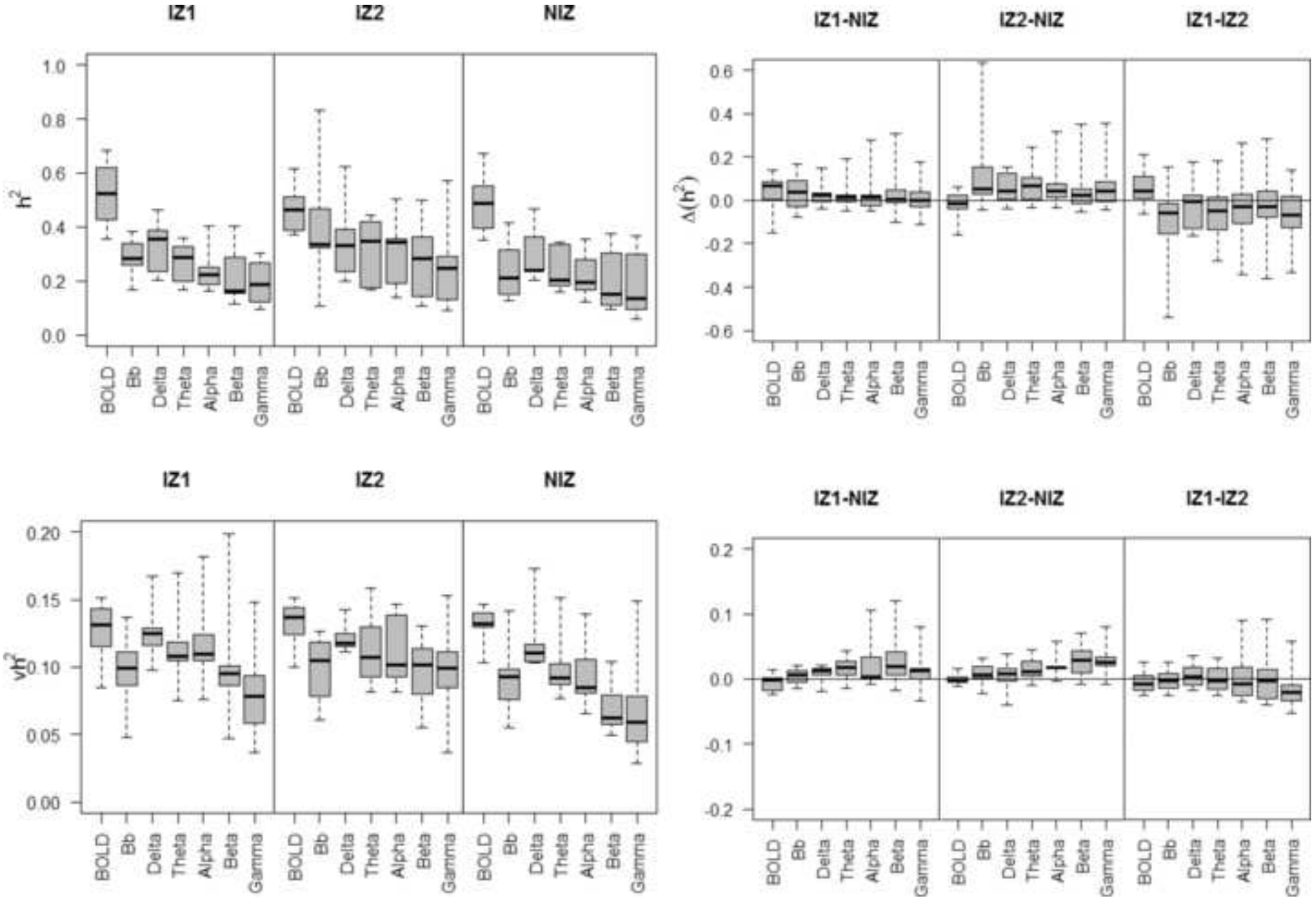

Table

Tables

Patient	Sex	Age (yrs)	Hand	Diagnosis	Onset (yrs)	Seizure Frequency	MRI	Surgical Resection	Outcome	
									ILAE	Months
P01	M	26	Right	Bi-Temporal	7	Monthly	L. HS	L. TL	I	38
P02	F	31	Right	Temporal	6	Weekly	NL	L. TL	IV	43
P03	M	28	Right	Frontal	12	Daily	FCD L. SFG\ MFG	L. SFG/MFG Sup. SMA	I	22
P04	M	38	Right	Frontal	8	Daily	L HS*	R. SMA, m. SFG	I	23
P05	F	34	Right	Frontal	7	Daily	FCD L. IFG	L. SFG/MFG	I	19
P06	F	27	Left	Frontal	3	Daily	NL	L. SFG	I	24
P07	M	24	Right	Temporal	15	Weekly	NL	R.TL	IV	19
P08	M	34	Right	Frontal	9	Daily	FCD L. MFG	L.MFG/IFG	I	11
P09	M	32	Right	Frontal	16	Weekly	NL	R. OrbF/IFG	I	22

Table 1: Patient Clinical Demography. *Abbreviations:* yrs=years, Hand.=Handedness, M=male, F=female, R=right, L=left, NL=non-lesional, HS=hippocampal sclerosis, FCD=focal cortical dysplasia, SFG=superior frontal gyrus, MFG=middle frontal gyrus, IFG=inferior frontal gyrus, TL=temporal lobe, Sup.= superior, SMA= supplementary motor area, OrbF=orbitofrontal gyrus. *ILAE surgery outcome:* I: Completely seizure free, no aura; II: Only auras, no other seizures; III: One or two seizure days per years, ± auras; IV: Four seizure days per year to 50% reduction of baseline seizure days, ± auras; V: Less than 50% reduction of baseline seizure days to 100% increase of baseline seizure days, ± auras; VI: More than 100% increase of baseline seizure days, ± auras. *Hippocampal sclerosis was considered incidental in this patient. Ictal SPECT, PET, MEG and scalp EEG all support a right frontal seizure origin.

	Clinical Electrophysiological Zone					
	EZ/IZ1		IZ2		NIZ	
Total No. of ROIs	88		86		396	
Total Pairwise Interactions	410		478		10655	
	Grids	**Depth**	**Grid**	**Depth**	**Grid**	**Depth**
P01	0	8	0	8	0	14
P02	0	8	10	4	38	0
P03	13	0	0	6	43	12
P04	0	8	0	13	0	11
P05	8	7	8	0	54	4
P06	9	0	4	0	71	0
P07	6	6	20	0	19	6
P08	6	2	3	1	3	69
P09	0	7	0	9	0	52

Table 2 – Regions of interest/electrodes. Numbers of recording electrodes localized to each electrophysiological zone, overall (top) and for each participant (bottom). Pairwise interactions refers to functional connectivity estimates that contribute to the sample analysed at the group level, and include all possible interactions within each individual and each zone. Interactions between zones were not considered.

Metric	Modality		IZ1		IZ2		NIZ	
			BOLD h^2	BOLD vh^2	BOLD h^2	BOLD vh^2	BOLD h^2	BOLD vh^2
h^2	icEEG Bband	r	-	-	-	-0.2	0.09	-
		p	-	-	-	<.0001	<.0001	-
	Delta icEEG	r	0.16	-	-	-0.15	0.19	-
		p	0.0008	-	-	0.001	<.0001	-
	Theta icEEG	r	-	-	-	-0.17	0.13	-
		p	-	-	-	0.0002	<.0001	-
	Alpha icEEG	r	-	-	-	-0.18	0.11	-
		p	-	-	-	<.0001	<.0001	-
	Beta icEEG	r	-	-	-	-0.23	0.1	-
		p	-	-	-	<.0001	<.0001	-
	Gamma icEEG	r	-	-	-	-0.27	0.05	-
		p	-	-	-	<.0001	<.0001	-
vh^2	BOLD	r	-0.41		-0.26		-0.17	
		p	<.0001		<.0001		<.0001	
	icEEG Bband	r	-	-	-	-	0.14	-
		p	-	-	-	-	<.0001	-
	Delta icEEG	r	-	-	-	-	0.18	-
		p	-	-	-	-	<.0001	-
	Theta icEEG	r	-	-	-	-	0.15	-
		p	-	-	-	-	<.0001	-
	Alpha icEEG	r	-	-	-	0.15	0.13	0.06
		p	-	-	-	0.001	<.0001	<.0001
	Beta icEEG	r	-	-	-	-	0.08	0.05
		p	-	-	-	-	<.0001	<.0001
	Gamma icEEG	r	-	-	-	-	0.07	0.05
		p	-	-	-	-	<.0001	<.0001
IEDs		r	0.2	-	-	0.24	-	-
		p	<.0001	-	-	<.0001	-	-

Table 3 – Inter-modal connectivity correlation (Pearson's r) between connectivity metrics. Correlations considered significant at a Bonferroni-corrected level $p<0.002$. Abbreviations: Bband, broadband; Mn, mean.

Metric	Modality	Whole Model (14)	Patient (8)	Mean IEDs (11531)	Euclid. Dist. (11531)	Elec. Type (2)	Zone (2)
h^2	**BOLD**	190.4	208.6	4.9	67.9	-	13.5
	icEEG Bband	453.5	265.2	-	812.2	378	47.9
	Delta icEEG	357.3	46.4	70.2	261.3	85.2	20.1
	Theta icEEG	219.5	44.1	21.8	421.1	123.2	40.5
	Alpha icEEG	164.7	57.67	-	262.3	165.2	33.81
	Beta icEEG	318.2	47.7	9.2	299	203.4	30.43
	Gamma icEEG	443.5	244.1	131.3	209.8	165.7	52.5
vh^2	**BOLD**	35.9	54.7	10,	7.6	-	3.9
	icEEG Bband	839.1	471.5	-	260.2	195.3	21.5
	Delta icEEG	437	194.5	16	113	96.4	4.2
	Theta icEEG	639.7	292.4	226.1	135.8	176.2	15.35
	Alpha icEEG	571.8	239	330.6	72.2	340.3	44.1
	Beta icEEG	739.3	161.8	792.3	218.6	401.9	88.3
	Gamma icEEG	1136.7	604.2	140.7	200.8	444.7	182.6

Table 4. Significant main effects (F) Numbers in brackets indicate degree of freedom. Significant to $p<0.007$, non-significant effects indicated by a dash(-).

Metric	Modality		IZ1	IZ2	NIZ
h^2	BOLD	Mn	0.51	0.45	0.47
		SD	0.20	0.17	0.17
	icEEG Bband	Mn	0.20	0.29	0.22
		SD	0.20	0.23	0.17
	Delta icEEG	Mn	0.25	0.30	0.29
		SD	0.17	0.18	0.15
	Theta icEEG	Mn	0.19	0.27	0.24
		SD	0.16	0.17	0.14
	Alpha icEEG	Mn	0.20	0.27	0.23
		SD	0.15	0.16	0.13
	Beta icEEG	Mn	0.19	0.25	0.20
		SD	0.16	0.16	0.13
	Gamma icEEG	Mn	0.19	0.26	0.19
		SD	0.16	0.17	0.15
vh^2	BOLD	Mn	0.13	0.13	0.13
		SD	0.04	0.04	0.04
	icEEG Bband	Mn	0.09	0.10	0.09
		SD	0.04	0.03	0.04
	Delta icEEG	Mn	0.12	0.12	0.12
		SD	0.03	0.03	0.04
	Theta icEEG	Mn	0.10	0.11	0.10
		SD	0.03	0.03	0.03
	Alpha icEEG	Mn	0.10	0.11	0.10
		SD	0.04	0.04	0.03
	Beta icEEG	Mn	0.08	0.09	0.07
		SD	0.04	0.03	0.03
	Gamma icEEG	Mn	0.07	0.09	0.06
		SD	0.04	0.04	0.03

Table 5 h^2 and vh^2 estimates by zone for each modality

	Dependant Variable	IZ1-IZ2 (1)	IZ1-NIZ (1)	IZ2-NIZ (1)
h^2	**BOLD**	25.4	16.8	4*
	icEEG Broadband	82	6.6*	70.9
	Delta icEEG	33.8	30.7	-
	Theta icEEG	80	40	20.4
	Alpha icEEG	64	11.3	40.2
	Beta icEEG	51.8	3.9*	45.5
	Gamma icEEG	58.9	-	100.9
Var_h^2	**BOLD**	-	7.7	-
	icEEG Broadband	25.8	-	40.7
	Delta icEEG	4.2*	-	8.3
	Theta icEEG	24.3	-	24.9
	Alpha icEEG	29.2	7.9	7.9
	Beta icEEG	60.8	14.4	176.6
	Gamma icEEG	146.6	19	364.5

Table 6 - Significant post-hoc t-contrasts for Zone (F) numbers in brackets indicate degree of freedom. Non-significant test marked with dash (-), significant at $p<0.05$ marked with asterix (*), al others significant at bonferonni-corrected level of $p<0.007$.